# Supplementary Information

# Electrochemiluminescence amplification in bead-based assays induced by a freely diffusing iridium(III) complex

Emily Kerr[1,*], Sara Knezevic[2], Paul S. Francis[3], Conor F. Hogan[4], Giovanni Valenti[5], Francesco Paolucci[5], Frédéric Kanoufi[6], Neso Sojic[2,*]

[1] Institute for Frontier Materials, Deakin University, Geelong, Victoria 3220, Australia.

[2] Univ. Bordeaux, CNRS, Bordeaux INP, Institut des Sciences Moléculaires, UMR 5255, 16 avenue Pey-Berland, 33607 Pessac, France.

[3] School of Life and Environmental Sciences, Deakin University, Geelong, Victoria 3220, Australia.

[4] Department of Biochemistry and Chemistry, Biomedical and Environmental Sensor Technology centre, La Trobe Institute for Molecular Science, La Trobe University, Melbourne, Victoria 3086, Australia.

[5] Department of Chemistry "Giacomo Ciamician", University of Bologna, 40126 Bologna, Italy.

[6] Université Paris Cité, ITODYS, CNRS, F-75013 Paris, France

[*] To whom correspondence should be addressed: emily.kerr@deakin.edu.au; sojic@u-bordeaux.fr

**Image Analysis**

Where unspecified, contrast is automatically adjusted by ImageJ. False color was applied to micrographs using Green (for PL) and Red (for ECL) look up tables in ImageJ. For each micrograph, a 180×4 pixel rectangle, centered at the base (side-view, 71.4×1.6 μm) or center (top-view 45.7×1.0 μm) of the bead, was used to generate the emission profile using the default profile settings of the ImageJ software; the average pixel intensity of the width of the rectangle (four pixels) was plotted over a 180 pixel window. For top-view experiments, background-subtracted ECL intensities were calculated by subtracting the maximum emission from the first 10 pixels (where no emission from the bead was observed) from the maximum ECL signal from the entire ECL profile (Figure S5).

The distance dependent background ECL profile of the emission from $[Ir(sppy)_3]^{3-}$ complicated the calculation of the ECL emission profile from Ru@PS beads due to the 'blocking' effect of the PS beads and angle of the microscope objective (described in detail below and in the SI) in the side-view orientation. To accurately compensate for the change in ECL emission from $[Ir(sppy)_3]^{3-}$, both with distance from the WE surface and in the presence of the Ru@PS beads, we determined the $[Ir(sppy)_3]^{3-}$ emission profile from a 'bare' (unfunctionalized) PS bead in the presence of $[Ir(sppy)_3]^{3-}$. The profile was normalized to the intensity of each micrograph using a procedure described in detail in Figure S6. We also collected the emission profiles from bare beads in top-view configuration and found that this effect did not substantially impact the ECL intensity profiles in this configuration (Figure S11 and Table S1).

(1) $[Ru(bpy)_3]^{2+} - e^- \rightarrow [Ru(bpy)_3]^{3+}$

(2) $TPrA - e^- \rightarrow TPrA^{\bullet+}$

(3) $[Ru(bpy)_3]^{3+} + TPrA \rightarrow [Ru(bpy)_3]^{2+} + TPrA^{\bullet+}$

(4) $TPrA^{\bullet+} \rightarrow TPrA^{\bullet} + H^+$

(5) $[Ru(bpy)_3]^{3+} + TPrA^{\bullet} \rightarrow [Ru(bpy)_3]^{2+}* + \text{other products}$

(6) $[Ru(bpy)_3]^{2+} + TPrA^{\bullet} \rightarrow [Ru(bpy)_3]^{+} + \text{other products}$

(7) $[Ru(bpy)_3]^{+} + [Ru(bpy)_3]^{3+} \rightarrow [Ru(bpy)_3]^{2+}* + [Ru(bpy)_3]^{2+}$

(8) $[Ru(bpy)_3]^{+} + TPrA^{\bullet+} \rightarrow [Ru(bpy)_3]^{2+}* + TPrA$

(9) $[Ru(bpy)_3]^{2+}* \rightarrow [Ru(bpy)_3]^{2+} + h\nu$

**Scheme S1:** Mechanism of homogeneous $[Ru(bpy)_3]^{2+}$ and TPrA co-reactant ECL.

(10) $TPrA - e^- \rightarrow TPrA^{\bullet+}$

(11) $TPrA^{\bullet+} \rightarrow TPrA^{\bullet} + H^+$

(12) $[Ru(bpy)_3]^{2+} + TPrA^{\bullet} \rightarrow [Ru(bpy)_3]^{+} + \text{other products}$

(13) $[Ru(bpy)_3]^{+} + TPrA^{\bullet+} \rightarrow [Ru(bpy)_3]^{2+}* + TPrA$

(14) $[Ru(bpy)_3]^{2+}* \rightarrow [Ru(bpy)_3]^{2+} + h\nu$

**Scheme S2:** Heterogeneous $[Ru(bpy)_3]^{2+}$ and TPrA co-reactant ECL pathway. In this heterogeneous format, $[Ru(bpy)_3]^{2+}$ is immobilized on an insulating entity (bead, cell, etc.) and not directly oxidized at the electrode surface.

(15) $TPrA - e^- \rightarrow TPrA^{\bullet+}$

(16) $TPrA^{\bullet+} \rightarrow TPrA^{\bullet} + H^+$

(17) $[Ir(sppy)_3]^{3-} - e^- \rightarrow [Ir(sppy)_3]^{2-}$

(18) $Ru(bpy)_3]^{2+} + TPrA^{\bullet} \rightarrow [Ru(bpy)_3]^{+} + \text{other products}$

(19) $[Ru(bpy)_3]^{+} + [Ir(sppy)_3]^{2-} \rightarrow [Ru(bpy)_3]^{2+}* + TPrA$

(20) $[Ru(bpy)_3]^{2+}* \rightarrow [Ru(bpy)_3]^{2+} + h\nu$

**Scheme S3:** Proposed redox-mediator ($[Ir(sppy)_3]^{3-}$) enhanced $[Ru(bpy)_3]^{2+}$ and TPrA co-reactant ECL pathway.

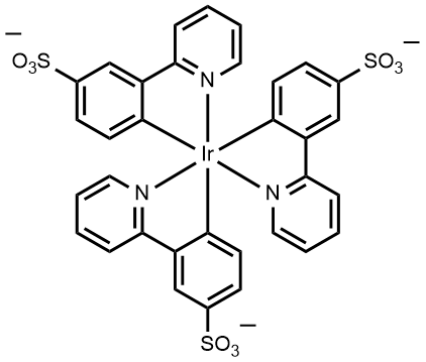


**Figure S1:** Structure of $[Ir(sppy)_3]^{3-}$.

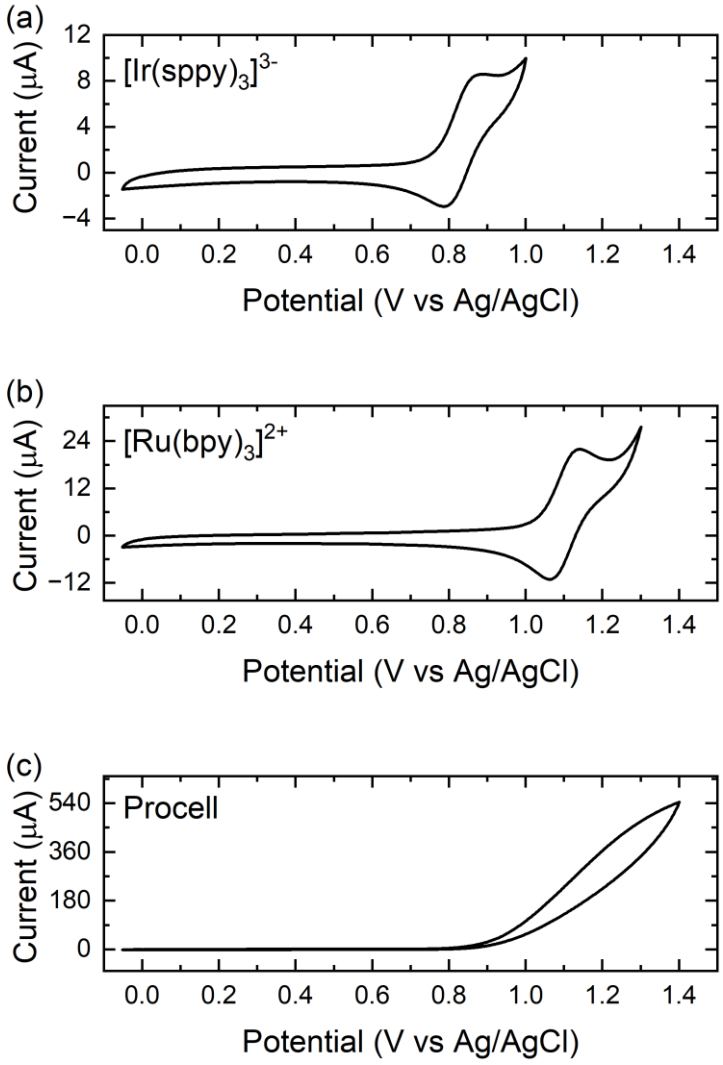


**Figure S2:** Cyclic voltammograms of (a) 1 mM $[Ir(sppy)_3]^{3-}$ in 0.1 M phosphate buffer, pH 7.5, (b) 1 mM $[Ru(bpy)_3]^{2+}$ in 0.1 M phosphate buffer, pH 7.5, (c) Procell solution. Scan rate: 0.1 V/s. Reproduced from Ref. 1 with permission from the Royal Society of Chemistry.[1]

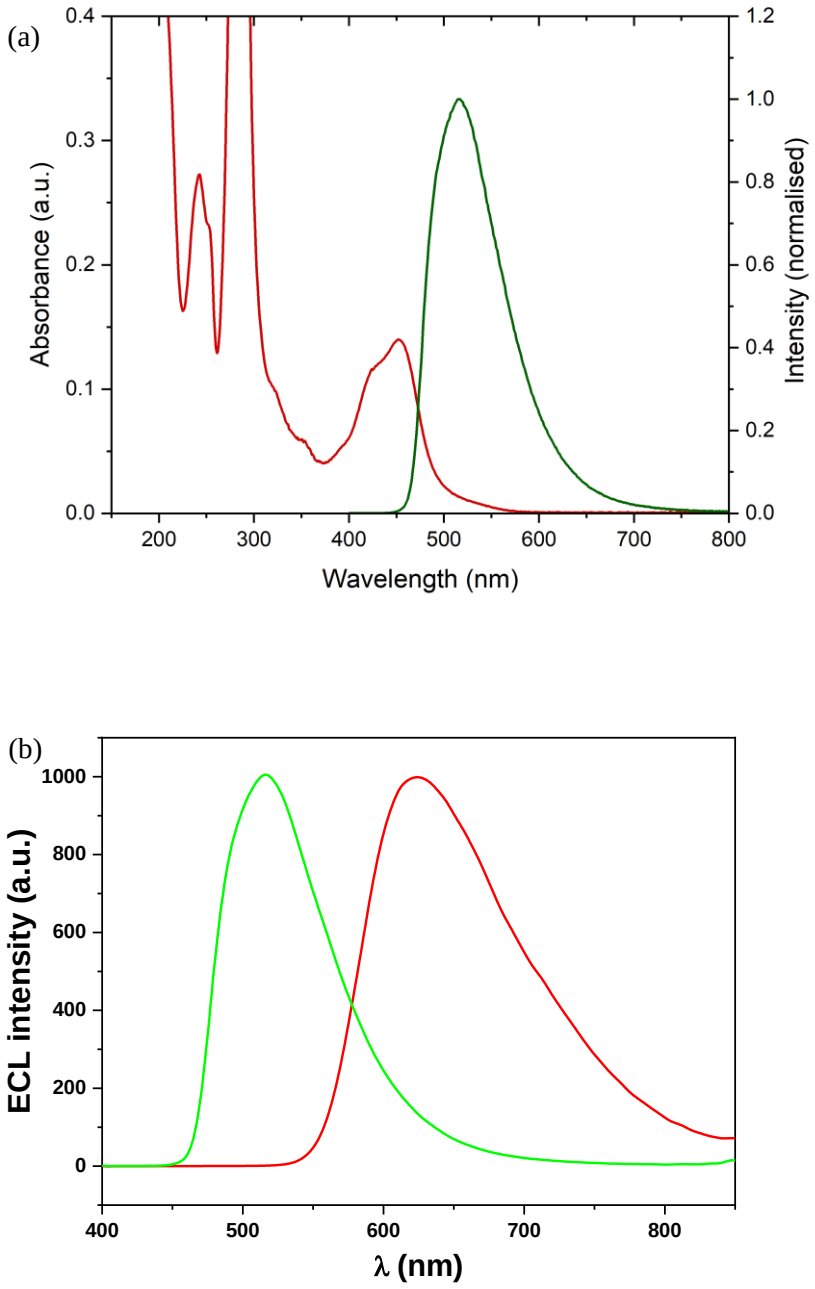


**Figure S3:** (a) UV-visible absorption spectrum of $[Ru(bpy)_3]^{2+}$ (red plot) and normalized photoluminescence emission spectrum of $[Ir(sppy)_3]^{3-}$. Complex concentration 10 μM in ultra-pure (Milli-Q) water at ambient temperature. Reproduced from Ref. 1 with permission from the Royal Society of Chemistry.[1] (b) Normalized ECL spectra of $[Ir(sppy)_3]^{3-}$ (green plot) and $[Ru(bpy)_3]^{2+}$ (red plot) in Procell with 100 μM of the luminophore at 1.2 V. Similar ECL spectra were obtained for $[Ru(bpy)_3]^{2+}$ in solution and when immobilized on the PS beads.

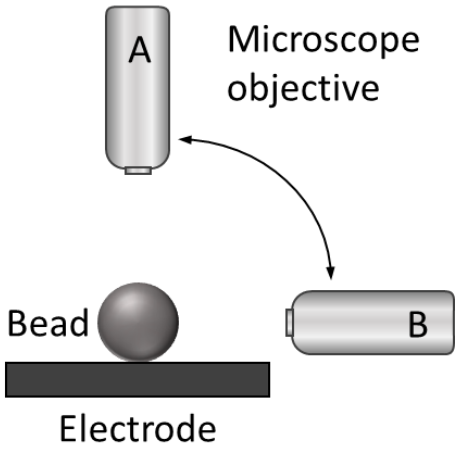


**Figure S4:** Schematic representation of top, 63× objective (A) and side, 40× objective (B) configurations used in ECL microscopy.

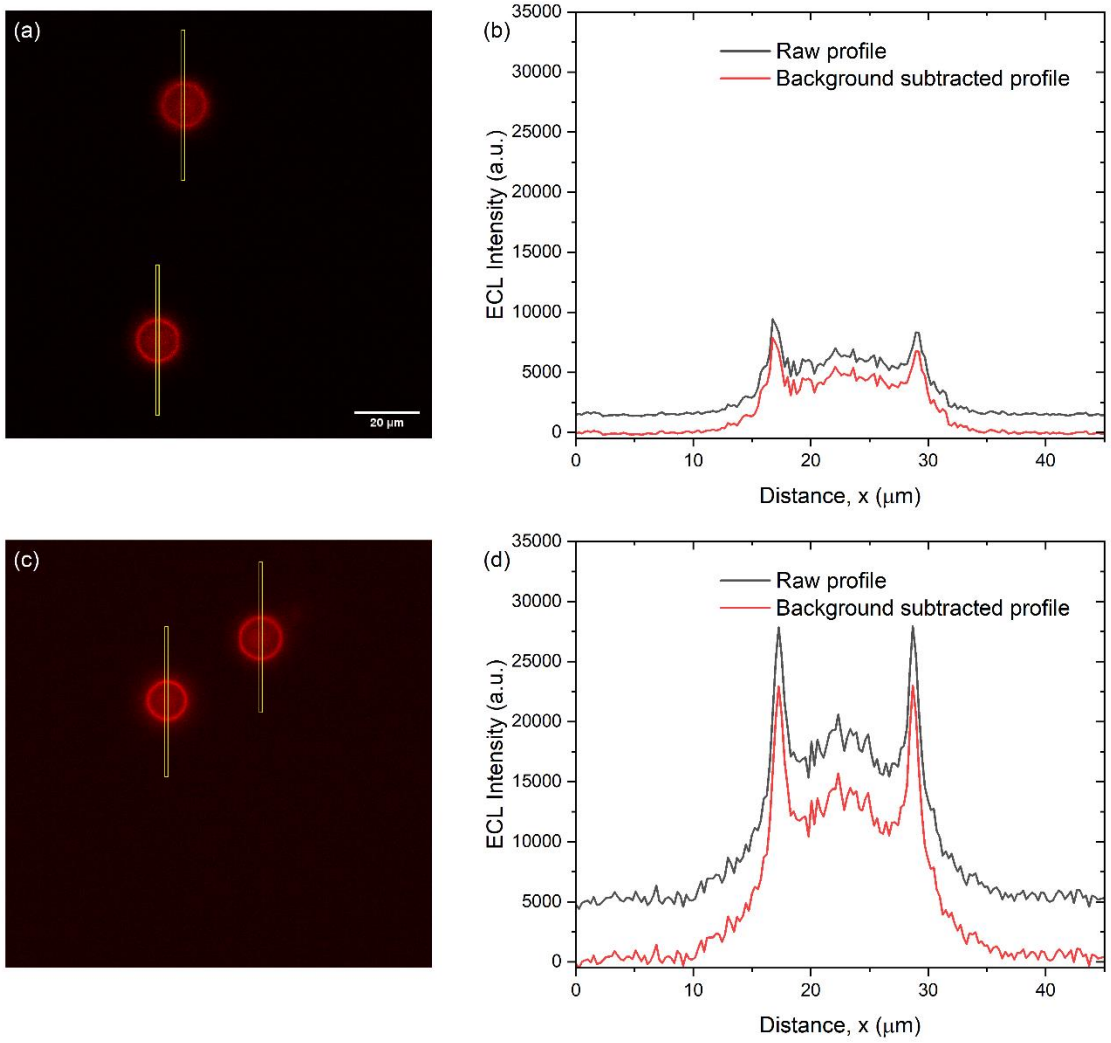


**Figure S5:** Representative ECL micrographs (top-view configuration) obtained in Procell (a) and Procell with 100 µM $[Ir(sppy)_3]^{3-}$ (c), including 180×4 pixel rectangles (shown in yellow) used to generate ECL emission profiles (b and d respectively), 1.2 V, 1 s CA pulse, 2 s EM-CCD exposure time. To generate the background subtracted profiles (red lines, b and d) the maximum of the first 10 pixels (~2.54 µm) of ECL emission (where no emission from Ru@PS was observed) was subtracted from the raw profile (black lines, b and d).

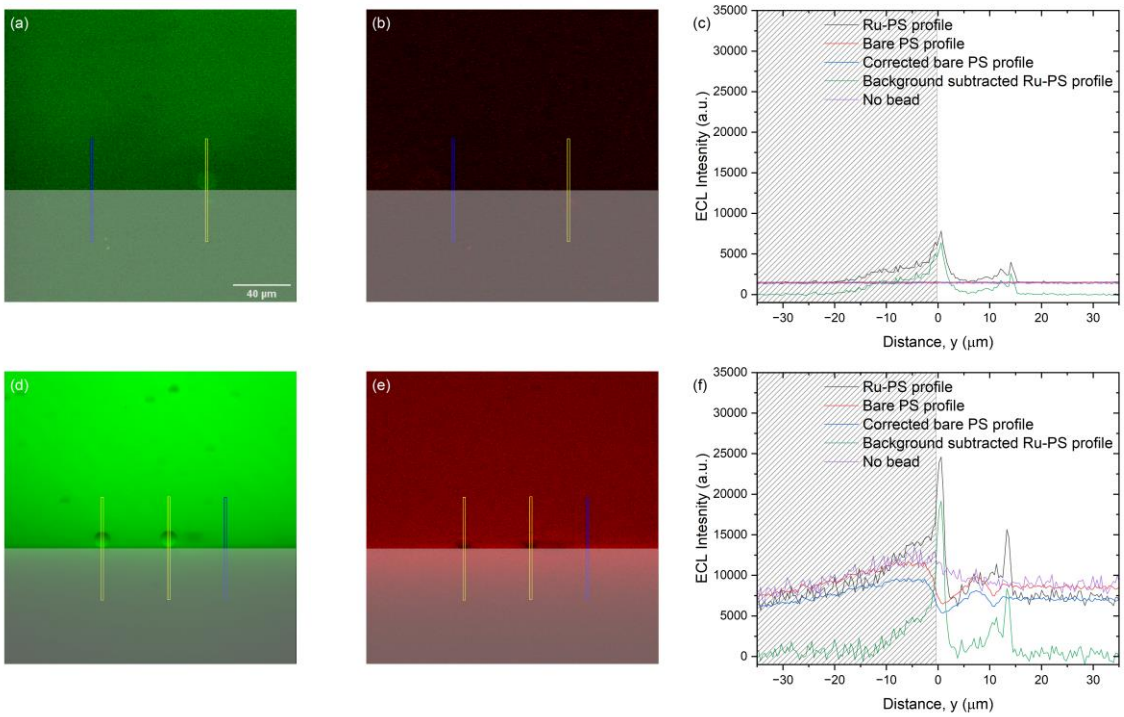


**Figure S6:** Representative side-view configuration PL micrographs (a and d) and corresponding ECL micrographs (b and e) obtained in Procell (a and b) and Procell with 100 µM $[Ir(sppy)_3]^{3-}$ (d and e) including shaded zone representing reflection of ECL on the electrode surface ($z < 0$ µm) 180×4 pixel rectangles (shown in yellow) used to generate ECL emission profiles (c and f, respectively) of unlabeled PS beads in side-view configuration at 1.2 V (2 s CA pulse, EM-CCD exposure 3 s), hatched zone represents reflection of ECL on the electrode surface ($z < 0$ µm). Blue rectangles, away from the PS spheres, show the background ECL profile; i.e. from $[Ir(sppy)_3]^{3-}$ in solution only (purple lines in figures c and f). To generate the background subtracted profiles (green lines, c and f) the maximum of the first 10 pixels (~3.97 µm) of ECL emission (where no emission from Ru@PS was observed) was calculated for both Ru@PS (black lines) and bare PS (red lines) profiles. A correction factor was applied to the bare PS profile (blue lines) to normalize the bare PS profile to the Ru@PS profile. This corrected bare PS profile was then subtracted from the raw Ru@PS profile to generate the background subtracted Ru@PS profile (green lines).

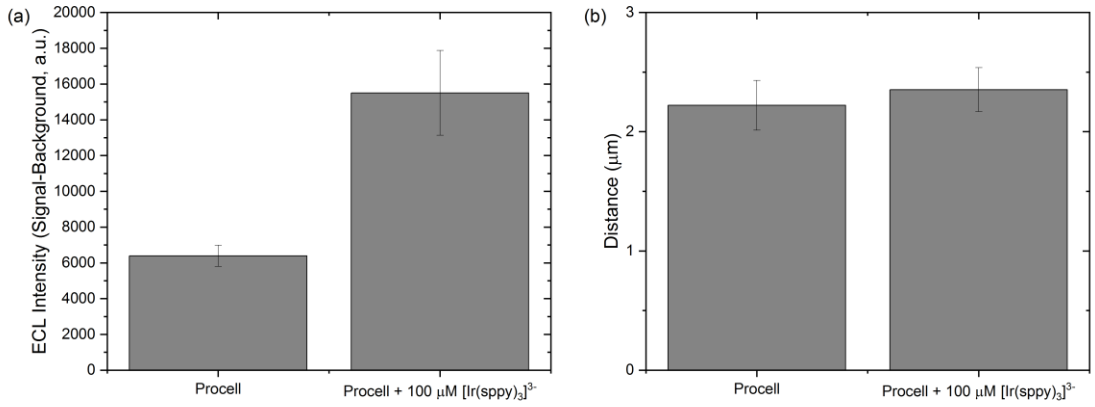


**Figure S7:** (a) ECL intensities obtained at 1.2 V, 2 s CA pulse, EM-CCD exposure 3 s, side-view configuration (n = 4 electrodes). (b) thickness of the ECL emission layer; a Y5 emission filter (Leica, 11525312, λ emission: 662.5 to 737.5 nm) was used to selectively monitor ECL from $[Ru(bpy)_3]^{2+}$; distance was calculated as the mean width of the ECL layer at the half-maximum (extracted from the ECL profiles) as described previously (n = 4 electrodes).[2]

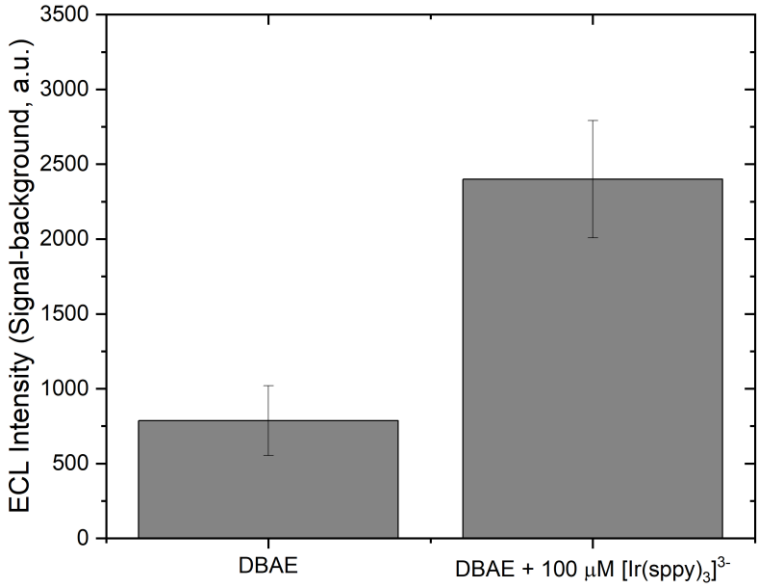


**Figure S8:** ECL intensities obtained at 1.2 V in 0.1 M, pH 7.4 phosphate buffer with 20 mM DBAE (pulse time 15 s, EM-CCD exposure 16 s, n = 6 electrodes).

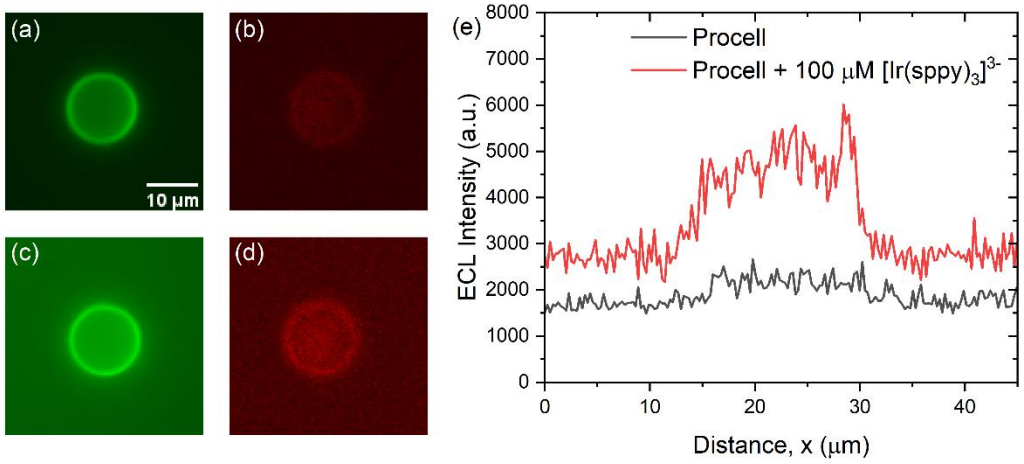


**Figure S9:** Top-view configuration micrographs of 12 µm Ru@PS beads using PL (a and c, green images, contrast scale 0 to 15,000) and ECL mode (b and d, red images contrast scale 0 to 10,000). Figures a-b obtained in 0.1 M pH 7.4 phosphate buffer with 20 mM DBAE, c-d obtained in 0.1 M pH 7.4 phosphate buffer with 20 mM DBAE with 100 µM $[Ir(sppy)_3]^{3-}$, 1.2 V, CA pulse 15 s, EM-CCD exposure 16 s. (e) Representative profiles of ECL intensity of Ru@PS beads at 1.2 V (15 s CA pulse) in 0.1 M pH 7.4 phosphate buffer with 20 mM DBAE and pH 7.4 phosphate buffer with 20 mM DBAE with 100 µM $[Ir(sppy)_3]^{3-}$.

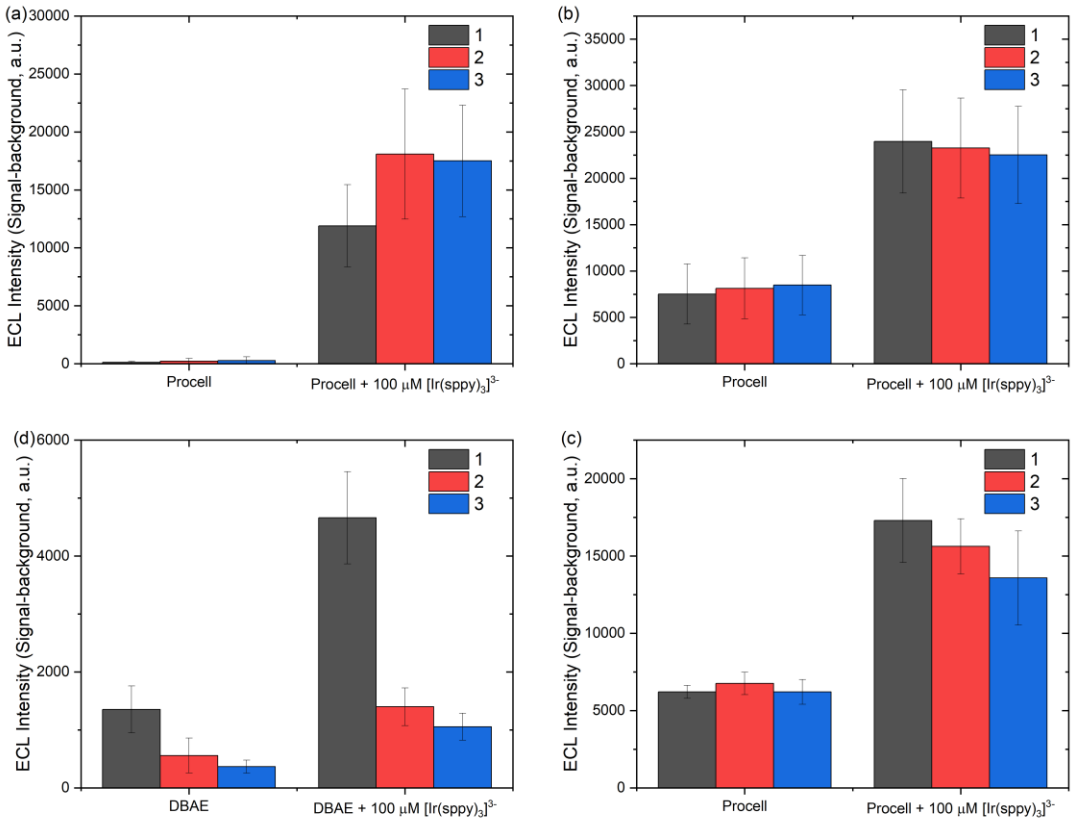


**Figure S10:** Change in ECL signal from three subsequent pulses: (a) top-view configuration, 0.9 V, 4 s CA pulse, 5 s EM-CCD exposure time; (b) top-view configuration, 1.2 V, 1 s CA pulse, 2 s EM-CCD exposure time; (c) 20 mM DBAE in 0.1 M pH 7.4 phosphate buffer, top-view configuration, 1.2 V, 15 s CA pulse, 16 s EM-CCD exposure time; and (d) side-view configuration, 1.2 V, 2 s CA pulse 3 s EM-CCD exposure time.

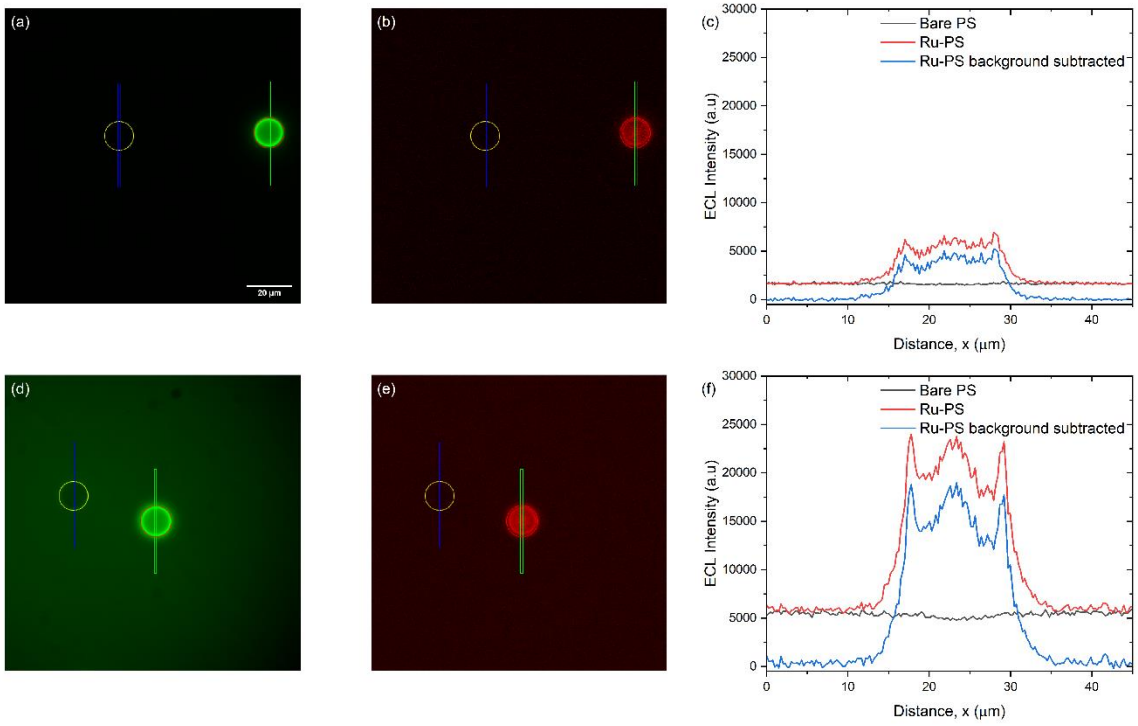


**Figure S11:** Representative top-view configuration PL micrographs (a and d) and ECL micrographs (b and e) obtained in Procell (a and b), and Procell with 100 µM $[Ir(sppy)_3]^{3-}$ (d and e) including 180×4 pixel rectangles (shown in blue and green) used to generate ECL emission profiles (c and f, respectively) of bare PS beads (circled in yellow) and Ru@PS beads (circled in red) 1.2 V, 1 s CA pulse, EM-CCD exposure 2 s. To generate the bare-PS background subtracted profiles (blue lines, c and f) the bare PS profile (black lines, c and e) was subtracted from the raw Ru@PS profile (red lines, c and f).

**Table S1:** Top-view ECL intensities with and without correction for bare PS profile (average of n = 2 electrodes).

| | Procell | Procell + 100 µM $[Ir(sppy)_3]^{3-}$ |
|---|---|---|
| 0.9 V | | |
| Signal-Background (a.u.) | 727 | 8845 |
| Signal-Background, bare PS (a.u.) | 754 | 8721 |
| Difference (%) | -4% | 1% |
| 1.2 V | | |
| Signal-Background (a.u.) | 5342 | 18300 |
| Signal-Background, bare PS (a.u.) | 5344 | 19128 |
| Difference (%) | 0% | -5% |

As shown in Table S1, minimal difference was observed between the ECL signals calculated using background subtraction with or without correction for bare bead in the top view configuration. Therefore, for all analyses in top-view configuration, background correction was conducted as per the procedure outlined in the experimental section, and further detailed in Figure S6.

**References**

1. Kerr, E.; Hayne, D. J.; Soulsby, L. C.; Bawden, J. C.; Blom, S. J.; Doeven, E. H.; Henderson, L. C.; Hogan, C. F.; Francis, P. S., A redox-mediator pathway for enhanced multi-colour electrochemiluminescence in aqueous solution. *Chem. Sci.* **2022,** *13* (2), 469-477.
2. Fiorani, A.; Han, D.; Jiang, D.; Fang, D.; Paolucci, F.; Sojic, N.; Valenti, G., Spatially resolved electrochemiluminescence through a chemical lens. *Chem. Sci.* **2020,** *11* (38), 10496-10500.